Forces shaping a Hox morphogenetic gene-network

Sol Sotillos[1], Mario Aguilar[1] and James Castelli-Gair Hombría*

CABD, CSIC/JA/Universidad Pablo de Olavide, 41013 Seville, Spain

Classification: Biological Sciences, Developmental Biology

Short title: Shaping of a morphogenetic gene-network

Key words: Cv-c, RhoGAP, morphogenesis, evolution, gene-network

1 Co-first author

*Correspondence to: jcashom@upo.es

ABSTRACT:

The Abdominal-B selector protein induces the organogenesis of the posterior spiracles by coordinating an organ specific gene-network. The complexity of this network begs the question of how it originated and what were the selective pressures driving its formation. As the network probably formed piecemeal with elements being recruited sequentially, we studied the consequences of expressing individual effectors of this network in naive epithelial cells. We find that, except with expression of the Cv-c RhoGAP protein, most effectors have little morphogenetic effect by themselves. In contrast, Cv-c expression causes cell motility and downregulates epithelial polarity and cell adhesion proteins. These effects differ in cells endogenously expressing Cv-c because they have acquired compensatory mechanisms. In spiracle cells, the downregulation of polarity and E-Cadherin expression caused by Cv-c induced Rho1 inactivation are compensated by the simultaneous spiracle upregulation of GEF proteins, cell polarity and adhesion molecules. Other epithelial cells, which also have coopted Cv-c to their morphogenetic gene-networks are also resistant to Cv-c's deleterious effects. We propose that cooption of a new morphogenetic regulator to a selector cascade causes cellular instability, resulting in a strong selective pressure that leads that same cascade to recruit molecules that compensate it. To our knowledge, this is the first experimental based hypothesis proposing how the frequently observed complex organogenetic gene-networks are put together.

\body

Organogenesis is directed by the activation of gene regulatory networks in specific positions of the embryo. In *Drosophila,* three well studied models include the posterior spiracles where the organogenesis gene-network is activated downstream of the Hox selector protein Abdominal-B [Abd-B, (1)]; the salivary glands activated by Sex combs reduced [Scr, (2)]; and the tracheae where the network is activated by Trachealess (Trh) and Ventral veinless [Vvl, (3)]. Although these three organs are morphologically and functionally different, they have in common that a complex gene-network of intermediate transcription factors and signalling molecules modulate a similar combination of cell adhesion, cell polarity and cytoskeleton realizators. As these gene-networks probably formed piecemeal with elements of the network being recruited sequentially during organ evolution, two different scenarios can be envisaged. In one, the selective pressure to recruit each of the elements of the cascade is entirely driven by external environmental factors. In the second, although an external selective pressure may have acted as the initial trigger for the organ formation, endogenous physiological and developmental constraints would later have been used to shape the network by influencing what is developmentally stable and what is not.

Using as a model the morphogenesis of the posterior spiracles, we study how the activity of particular genes in the Abd-B network affects epithelial cell behaviour and how this may have influenced the modulation of other existing genes of the network or even resulted in the recruitment of new genes into it.

RESULTS AND DISCUSSION

The downstream effectors of the Abd-B posterior spiracle cascade include the RhoGTPase regulators RhoGEF64C, RhoGEF2 and the RhoGAP Crossveinless-c (Cv-

c), which control the cytoskeletal organization during spiracle morphogenesis ((1, 4, 5) Fig 1A). The cascade also activates various non-classical cadherins, stabilizes the protein levels of E-Cadherin (E-Cad) and upregulates the transcription of the apical cell polarity determinant Crumbs (Crb) [Fig 1A and (1)].

To test what is the contribution of each effector to spiracle morphogenesis, we expressed them individually in epithelial cells where they are normally not expressed or are expressed a lower levels than in the spiracle. This was achieved using either the epithelial ubiquitous *69B-Gal4* driver or the posterior compartment specific *en-Gal4* line. We observe that individual expression of RhoGEF2, RhoGef64C, E-Cad, Cad74A or Cad86C has little effect on epithelial cell behaviours (Fig 1 B-F, arrowheads). In contrast, Cv-cRhoGAP or Crb expression results in strong effects (Fig 1G, arrowhead). Crb is a key determinant of apical polarity and its overexpression has been shown to interfere with the apico-basal polarity generating a tissue collapse. As Crb induced effects are unrelated to normal tissue morphogenesis we did not study them any longer.

Cv-c is a RhoGAP protein required for Rho1 mediated actin reorganization (6, 7) that is activated transcriptionally in several morphogenetically active epidermal tissues including: the leading edge cells during embryo dorsal closure, the salivary gland primordia, the tracheal pits and the invaginating posterior spiracles (Fig S1A and (6)). As *cv-c* mutations result in morphogenetic abnormalities in all these tissues (6, 8, 9), we studied in detail this important epithelial morphogenetic regulator and its interactions with other downstream effectors of the Abd-B spiracle cascade.

Analysis of the ectoderm epithelial behaviour induced by *cv-c* expression.

To study the cellular morphogenetic effects controlled by this RhoGAP, we expressed *cv-c* ectopically in the posterior compartment of each segment from stage 11 onwards

using the *en-Gal4* line (Fig S1B-C). This allows us to compare the shape and behaviour of the normal non-expressing anterior compartment cells with that of neighbouring posterior compartment cells where we induced Cv-c. Expression of either Cv-c, or Cv-c fused to a C-terminal venusGFP tag, induces similar effects and were used indistinctly. As a negative control we expressed a Cv-c^{R601Q}-GFP protein where the critical catalytic Arginine 601 in the GAP domain is mutated to Glutamine. This mutation is present in the *cv-c*^{7} allele, which produces an inactive protein (6).

Expression of Cv-c^{R601Q}-GFP does not affect cell shape or the subcellular localization of ectodermal proteins like aPKC, Crb, E-Cad, Discs large (Dlg) or Scribble. These embryos develop into normal adult flies indicating that Cv-c^{R601Q}-GFP does not interfere with the endogenous Cv-c function (Fig 1I, arrowhead, 3B). In contrast, expression of *UAS-cv-c* or *UAS-cv-c-GFP* driven by *en-Gal4* results in lethality. In these embryos the Cv-c expressing cells change shape becoming up to 50% wider (Fig 1G'' and H compare with 1I''and J, quantified in SI materials and methods). In many cases stripes of Cv-c expressing cells from adjacent segments fuse, indicating that they either have increased motility or can displace the neighbouring wild type cells (19 out of 48 *en-Gal4>UAS-Cv-c* embryos have at least one segment fusion, Fig 1G and 3A lower panels). Cv-c expressing cells also show a strong downregulation of the apical polarity proteins aPKC and Crb (Fig 1G) and the adherens junction proteins E-Cad and ß-catenin (Fig 3C), while there is little effect on the expression levels of the basolateral septate junction markers Dlg, Scribble and Coracle (Fig 1G''-H, 3C).

As Cv-c has been shown to inactivate Rho1 (4, 7, 10, 11) we tested if the observed phenotypes are mimicked by Rho1 inactivation. Expression of the dominant negative Rho^{N19} with *en-Gal4* results in comparable phenotypes to expression of Cv-c-GFP (Fig 2B and Fig S2E). Simultaneous expression of Cv-c-GFP and the activated

Rho1^{V14} rescues the loss of aPKC, Crb and E-Cad (Fig 2D), restores normal cell shape and the cuticle defects caused by Cv-c (Fig S2C). In contrast, an activated form of Rac does not rescue the phenotypes caused by Cv-c, and the overexpression of a dominant negative Rac does not affect apical polarity protein distribution (Fig S3) confirming Cv-c's specificity for Rho1. These results indicate that the cell behaviours induced by ectopic Cv-c expression in the ectoderm are due to its expected function as a downregulator of Rho1 activity.

The loss of E-Cad and apical markers when expressing either Cv-c or Rho^{N19} does not cause massive cell death as demonstrated by the continuous presence of GFP expressing cells during embryogenesis and the modest levels of caspase 3 activity observed in this embryos (Fig 2E). Accordingly, the phenotypes caused by Cv-c are not recovered by coexpressing the anti-apoptotic protein DIAP1 (12) (Fig 2F).

These results show that recruitment of Cv-c to ectoderm epithelial cells has strong morphogenetic consequences, which may explain why it is transcriptionally activated in so many actively rearranging epithelial cells.

Cv-c expressing cells have a motile behaviour

To understand how Cv-c expression in the posterior compartment causes segment fusions, we studied the embryos *in vivo* and reconstructed the three dimensional organization of their epithelium. The *en-Gal4* line drives expression in the posterior compartment of each segment and every stripe is separated from those in other segments by anterior cells (Fig 3A upper panels, and sup. movie 1). Stripes of cells expressing the mutated Cv-c^{R601Q} protein are clearly separated from each other during development (Fig 1I, 3B). In contrast, in *en-Gal4 UAS-cv-c-GFP* embryos the Cv-c-GFP expressing cells exhibit a higher motility that can result in the occasional fusion of

en-Gal4 expressing stripes (Fig 3A lower panels, and sup. movie 2). The Cv-c expressing cells maintain tissue coherence indicating that the cells maintain cell adhesion despite the observed E-Cad downregulation (Fig 3C). While the motility of the cells is likely to be caused by Cv-c overexpression, the segment fusion may be Cv-c independent, as posterior compartments have similar cell affinities that favour their merge once they get in contact (13).

Three-dimensional analysis of fused segments reveals that the Cv-c expressing cells "crawl" over the anterior compartment cells that remain beneath them (Fig 1G, 3C-C' asterisks). Unlike control embryos (Fig 3D, 3E), the motile Cv-c cells become surrounded by high levels of the heparan sulphate proteoglycan Perlecan (Fig 3F, 3G), express ectopically the Mmp1 metalloprotease (Fig 3I compare with 3H) and upregulate the expression of LamininA (Fig 3K, compare with 3J). These results show that the Cv-c cells move cohesively over a newly formed extracellular matrix.

Tissue specific effects of Cv-c expression

We have shown that the specific Rho1 downregulation mediated by Cv-c's RhoGAP activity disrupts in the embryonic epithelium the normal levels of E-Cad and apical polarity proteins. Rho1 inactivation has been shown to cause similar effects in the eye epithelium and this has been interpreted as due to Rho1 being required to maintain adherens junctions during epithelial remodelling (14). While agreeing with this interpretation, we find our results puzzling as E-Cad, Crb and aPKC are present at high levels in the epithelial cells where *cv-c* is normally expressed (Fig S1A compare with Fig S1D,K,Q) (1, 15, 16). To test if the defects we observed could be explained by the Gal4 system expressing unusually high Cv-c levels with respect to the endogenous expression, we looked at the effects caused by Gal4 induced Cv-c overexpression in the

tissues expressing endogenous Cv-c. Even when overexpressing Cv-c with the spiracle specific line *ems-Gal4*, the ectopic Cv-c was unable to downregulate E-Cad, aPKC or Crb in the posterior spiracles (Fig 4B compare with A). Similarly, ectopic Cv-c in cells of the leading edge (Fig 4C, quantified in Fig S4), tracheal cells (Fig 4D) or the salivary glands (Fig 4E), causes no downregulation of apical markers or E-Cad. These data imply that the epithelial tissues that normally express *cv-c* respond differently to Cv-c, suggesting that they have compensatory mechanisms that allow the local downregulation of Rho1 without the loss of apical polarity and adhesion properties.

Abd-B recruits the compensatory mechanisms of the posterior spiracles

In the posterior spiracles, Abd-B activates besides *cv-c* various cadherins and polarity genes (Fig 1A). Especially interesting is the finding that, despite *crb* being ubiquitously expressed in all ectoderm cells, the Abd-B cascade reinforces *crb* transcription through a spiracle specific enhancer (1). To find out if the increased levels of Crb and cell adhesion protein upregulation in spiracles could be part of the compensatory mechanism, we studied if embryos heterozygous for these genes become more sensitive to Cv-c levels. Expression of Cv-c in the spiracles of *crb* heterozygous mutants results in spiracles with frequent invagination defects and abnormal expression of polarity molecules (Fig 4H, 28% of embryos overexpressing Cv-c have spiracle defects in *crb* heterozygous embryos, n=53) whilst the Cv-c^{R601Q} protein has no effect (Fig 4F, n=84). The same phenomenon is observed in a heterozygous mutant background for *E-cad* (Fig 4I, 33%, n=109) or *aPKC* (23%, n=71) and RhoGef64C (20%, n=66) or RhoGEF2 (24%, n=55) all of which are modulated by the Abd-B cascade in the posterior spiracles.

To find out if the Abd-B posterior spiracle gene-network includes compensatory mechanisms to ameliorate Cv-c effects on polarity and adhesion, we simultaneously

expressed ectopically Cv-c and Abd-B. We observe that expression of Abd-B rescues Cv-c epithelial defects in the areas associated to the formation of ectopic spiracles (Fig 4L-M). Similarly, we observe that ectopic expression of Abd-B is also capable of rescuing the defects caused by Rho1DN expression (Fig S5).

These results indicate that Abd-B controls a gene-network in the posterior spiracles that activates both Cv-c and the compensatory mechanism restricting the defects caused by Cv-c in the epithelium.

Compensation of Cv-c induced defects by expression of various cell proteins

The above data suggest that some of the posterior spiracle Abd-B targets can compensate for the defects caused by Cv-c downregulation of Rho. To identify what targets could be having a compensatory effect we tested if expression of any of the Abd-B spiracle effectors can rescue the defects caused by Cv-c in the epidermis.

GAP and GEF proteins have opposing regulation on Rho1 activation. While both RhoGEF2 and RhoGEF64C have been shown to function in the spiracle under the control of Abd-B, only RhoGEF2 expression is able to recover the membrane localization of both E-Cad (blue in Fig 5A, A' asterisks) and aPKC (Fig 5B in blue and B' asterisks). In our experiments RhoGEF64C does not localize to the membrane when expressed in the trunk with *en-Gal4* while RhoGEF2 does, suggesting why only RhoGEF2 is capable of compensating Cv-c defects in the epithelium.

We also tested if the outcome of Cv-c activation could be normalized by coexpression of E-Cad or aPKC, which are upregulated in the posterior spiracles (Fig.S1). When aPKC (a major regulator of apical polarity) is coexpressed with Cv-c, both aPKC (Fig 5C, blue) and E-Cad (Fig 5C red and C') localization to the membrane is recovered (Fig 5C´ arrowhead and asterisk). However, when we coexpress E-Cad and

Cv-c, only E-Cad membrane localization is restored, while aPKC localization remains cytoplasmic (red in Fig 5D and D', arrowhead and asterisk).

The result showing that newly transcribed and translated E-Cad can localize normally to the membrane in Cv-c expressing cells, suggests that Cv-c may be perturbing E-Cad membrane recycling which is fundamental during normal development (17). In agreement with this expectation we do not detect high *E-cad* RNA expression levels in posterior spiracles despite the high E-Cad protein levels observed, suggesting there is higher E-Cad stability or increased recycling in the spiracles.

To see if increased endocytic membrane recycling could compensate some of the defects, we coexpressed Cv-c with the endocytic regulator Rab11. In this situation E-Cad and aPKC localization are strongly normalized in the dorsal region (Fig 5E, arrowheads and asterisks in E' and E''). Interestingly, we found there are higher Rab11 levels on the wild type posterior spiracles than in neighbouring tissues (Fig 5F, arrowhead). Abd-B is required for the increased spiracle Rab11 protein levels as these disappear in *Abd-B* mutant embryos, and ectopic Abd-B expression results in ectopic Rab11 levels in anterior segments (Fig 5 G,H, arrowheads). Moreover, in ectopically expressing Cv-c embryos the rescue in polarity caused by ectopic Abd-B expression is correlated with the appearance of higher levels of E-Cad and Rab11 in the areas where the ectopic spiracles are formed (Fig S6).

These results show that ectoderm expression of Cv-c causes cell polarity defects that can be compensated by reinforcing the expression of apical polarity components either by increased recycling or transcription. Our observation that Abd-B controls in the spiracles the levels of proteins capable of rescuing Cv-c defects in the ectoderm, explain why Abd-B can compensate for Cv-c epithelial defects.

Cv-c contribution to shaping organogenesis networks

The organogenesis of the salivary glands, the trachea and the posterior spiracles is induced by the Scr, Trh/Vvl and Abd-B selector proteins respectively (1-3, 18). Although the networks activated by these transcription factors differ significantly, they share common targets like *cv-c, crb* and *E-cad*. Among them *cv-c* has received more attention because it is regulated by transcriptional activation prior to the onset of the morphogenetic movements; it has the capacity to influence the actin cytoskeleton organization through Rho1 regulation; and its mutation causes invagination defects in these tissues (4, 8, 9). Although published data have shown that Cv-c is required for the normal invagination of these organs, our experiments indicate that by itself, Cv-c activation in the epithelium does not induce invagination, and that its resulting downregulation of Rho1 has collateral effects on the maintenance of epithelial polarity and adhesion. We propose that during organ evolution, the cooption of Cv-c for cytoskeletal rearrangements lead to perturbation of the epithelial maintenance, which required the reinforcement of general polarity and adhesion molecules in those cells to compensate for the deleterious collateral defects. Thus, the recruitment of a new downstream morphogenetic regulator by a gene-network can generate a selective pressure leading that network to recruit other genes or to modify the expression of the existing network genes to regain homeostasis. In the spiracles this was achieved trough *de novo* local transcriptional upregulation of *crb,* various cadherins, GEF regulators as well as stabilization of E-Cad and Rab11 among other proteins by the Abd-B cascade (1). In the trachea and salivary glands *crb* upregulation is also observed [(1, 15, 16) and Fig S1] suggesting that a similar process may have occurred downstream of Scr and Trh. We believe that during organ evolution such pressures will occur frequently, leading to the local modulation of proteins required for basic cell functions that explain

the common occurrence of tissue specific enhancers in otherwise ubiquitously expressed genes.

Materials and Methods

Embryos grown at 25^{o}C were fixed for cuticle preparations and antibody stainings using standard methods. We generated a mutant Cv-c^{R601Q} and a wild type C-terminal fusion to venus-GFP and expressed them using the *Gal4* system. We performed cell size quantifications and *in vivo* time-lapse movies. Full details on procedures, mutants, constructs and antibodies are described extensively in SI Materials and Methods.

Acknowledgements: We thank S. Campuzano, H. Skaer, B. Denholm for comments to the manuscript, Nicole Gorfinkield and J. Culi for advice in embryo filming and quantification and D. Bilder, C. Dahmann and P. Roth for reagents.
S.S. is a Ramón y Cajal Fellow, M.A. is an FPI fellow. This work was supported by the Spanish MICINN, Consolider, European Regional Development Fund and the Junta de Andalucía grants to J.C-G. H and SS.

References

1. Lovegrove B*, et al.* (2006) Coordinated control of cell adhesion, polarity and cytoskeleton underlies Hox-induced organogenesis in *Drosophila*. *Curr Biol* 16:2206-2216.
2. Panzer S, Weigel D, & Beckendorf SK (1992) Organogenesis in Drosophila melanogaster: embryonic salivary gland determination is controlled by homeotic and dorsoventral patterning genes. *Development (Cambridge, England)* 114(1):49-57.
3. Boube M, Llimargas M, & Casanova J (2000) Cross-regulatory interactions among tracheal genes support a co-operative model for the induction of tracheal fates in the Drosophila embryo. *Mechanisms of development* 91(1-2):271-278.
4. Simoes S*, et al.* (2006) Compartmentalisation of Rho regulators directs cell invagination during tissue morphogenesis. *Development (Cambridge, England)* 133(21):4257-4267.
5. Hu N & Castelli-Gair J (1999) Study of the posterior spiracles of *Drosophila* as a model to understand the genetic and cellular mechanisms controlling morphogenesis. *Developmental Biology* 214:197-210.
6. Denholm B*, et al.* (2005) crossveinless-c is a RhoGAP required for actin reorganisation during morphogenesis. *Development (Cambridge, England)* 132(10):2389-2400.
7. Sato D, Sugimura K, Satoh D, & Uemura T (2010) Crossveinless-c, the Drosophila homolog of tumor suppressor DLC1, regulates directional elongation of dendritic branches via down-regulating Rho1 activity. *Genes Cells* 15(5):485-500.

8. Brodu V & Casanova J (2006) The RhoGAP crossveinless-c links trachealess and EGFR signaling to cell shape remodeling in Drosophila tracheal invagination. *Genes Dev* 20(13):1817-1828.

9. Kolesnikov T & Beckendorf SK (2007) 18 wheeler regulates apical constriction of salivary gland cells via the Rho-GTPase-signaling pathway. *Dev Biol* 307(1):53-61.

10. Wong CM, Lee JM, Ching YP, Jin DY, & Ng IO (2003) Genetic and epigenetic alterations of DLC-1 gene in hepatocellular carcinoma. *Cancer Res* 63(22):7646-7651.

11. Healy KD*, et al.* (2008) DLC-1 suppresses non-small cell lung cancer growth and invasion by RhoGAP-dependent and independent mechanisms. *Mol Carcinog* 47(5):326-337.

12. Wang SL, Hawkins CJ, Yoo SJ, Muller HA, & Hay BA (1999) The Drosophila caspase inhibitor DIAP1 is essential for cell survival and is negatively regulated by HID. *Cell* 98(4):453-463.

13. Jacinto A*, et al.* (2000) Dynamic actin-based epithelial adhesion and cell matching during Drosophila dorsal closure. *Curr Biol* 10(22):1420-1426.

14. Warner SJ & Longmore GD (2009) Distinct functions for Rho1 in maintaining adherens junctions and apical tension in remodeling epithelia. *J Cell Biol* 185(6):1111-1125.

15. Xu N, Keung B, & Myat MM (2008) Rho GTPase controls invagination and cohesive migration of the Drosophila salivary gland through Crumbs and Rho-kinase. *Dev Biol* 321(1):88-100.

16. Letizia A, Sotillos S, Campuzano S, & Llimargas M (2011) Regulated Crb accumulation controls apical constriction and invagination in Drosophila tracheal cells. *J Cell Sci* 124:240-251.

17. Nishimura T & Takeichi M (2009) Remodeling of the adherens junctions during morphogenesis. *Current topics in developmental biology* 89:33-54.

18. Hombria JC & Lovegrove B (2003) Beyond homeosis--HOX function in morphogenesis and organogenesis. *Differentiation* 71(8):461-476.

Figure Legends

Figure 1. Epithelial cell behaviour after expression of single Abd-B effectors.

(A) Schematic representation of the Abd-B posterior spiracle regulatory cascade and its downstream effectors. (B-J) Epidermis of stage 14-15 *Drosophila* embryos in which the indicated effector was expressed using *en-Gal4*. In all colour panels the cells expressing the effector are labelled in green. (B) RhoGEF64C expression (green) does not affect cell shape or apical polarity markers (aPKC in B' and red in B). (C) Epidermal cells expressing RhoGEF2 have deeper segment grooves but the cells maintain position and polarity markers (aPKC in red and C'). Expression of E-Cad (D), Cad86C (E) or Cad74A (F) have no obvious effect in cell behaviour, aPKC membrane localization (red in D E F and D' E' F') or Dlg (blue in D E F). (G-H) Cv-c expression in epithelial cells normally not expressing it causes loss of the apical marker aPKC (G' and red in G) without much effect on the basolateral marker Dlg (G'' and blue in G). (H) Close-up of G'', arrowhead points at Cv-c expressing cells with changed shape. (I-J) Expression of the inactive Cv-c^{R801Q} (green) in the epidermis does not affect cell shape or polarity as shown by staining with anti-aPKC (I' and red in I) and anti-Dlg (I'' and blue in I). (J) Close-up of I'', arrowhead points at cells expressing Cv-c^{R801Q}. Alongside most panels we present a Z-section taken across the region indicated by the thin white line. In colour panels aPKC is red, GFP green and Dlg blue. Scale bar: 10μm. Anterior is left, dorsal is up. Arrowhead points at cells expressing the effector indicated in the panel.

Figure 2. Effect of Cv-c and Rho1 expression on epithelial cell behaviour.

(A-F) Epidermis of stage 14-15 *Drosophila* embryos in which the indicated constructs were expressed using *en-Gal4*. (A) Cv-c expression in epithelial cells normally not expressing it causes loss of aPKC (A'). (B) Expression of the dominant negative

Rho1^{N19} causes the same defects on aPKC expression (red in B and B'). (C) Expression of an active Rho1^{V14} results in exaggerated segmental grooves but does not affect apical markers (aPKC, C' and red in C). (D) Expression of Rho1^{V14} rescues the loss of apical cell polarity caused by Cv-c expression. Note that the apparent areas without aPKC expression (asterisks in D) are due to the exaggerated segmental grooves present in these embryos as seen in the Z-section shown under panel D'. (E-F) Defects caused by ectopic Cv-c are not due to cell death as Cv-c expression persists, with only moderately increases cell death levels as shown by anti-active caspase 3 staining (caspase 3* E' and red in E) and the phenotypes caused by Cv-c induction cannot be rescued by coexpression of the apoptosis inhibitor Diap1 (F, aPKC in red and M', YFP in green). Note occasional segment fusions. Dlg is shown in Blue in A-F. Alongside most panels we present a Z-section taken across the thin white line. Scale bar: 10μm. Anterior is left, dorsal is up.

Figure 3. Expression of Cv-c induces epithelial reorganization. (A) Time lapse movie showing the cell behaviour of engrailed cells expressing GFP (upper panels) or Cv-c (lower panels) during embryonic development. While wild-type cells maintain their position in the posterior of the segment, Cv-c expressing cells can move as a coherent tissue fusing in some cases to the neighbouring *engrailed* stripe.
(B-M) Epidermis of stage 14 embryos in which, the indicated UAS lines, were expressed using *en-Gal4* as a driver. (B) Epidermal cells expressing the inactive Cv-c^{R601Q} in the posterior compartment are distributed as a monolayer. (C) Posterior cells expressing Cv-c crawl over adjacent wild-type cells (Note in C' that the Cv-c expressing cells have downregulated E-Cad and are moving over the wild type anterior cells that still express normal levels of E-Cad, asterisk). (D-E) In control Cv-c^{R601Q}

expressing embryos Perlecan localizes to the mesoderm and along the cells going through dorsal closure. (F-G) Motile cells expressing Cv-c are surrounded by Perlecan. (H-I) Expression of Mmp1 metalloprotease in control and Cv-c expressing embryos (H'-I' and red in H-I). Expression of Laminin A in control (J), and Cv-c expressing embryos (K). In (J) and (K) sections through the ectoderm (J-K) and mesoderm (J'-K') level are shown. In (B, C, G, J and K) Z-sections along the thin white lines are shown. E-Cad red, Scribble blue are shown in B-C; Perlecan, metalloprotease 1 and Laminin A are shown in red in D-G, H-I and J-K respectively, YFP in green.
Scale bar: 10μm.

Figure 4. Tissue specific response to Cv-c activation. (A-E) Epidermal cells that normally express Cv-c do not lose apical polarity markers by increased Cv-c expression. Apical is labelled with aPKC in red and basolateral in blue with either Dlg (A, C, E) or neurotactin (B). (A) Wild type stage 16 embryo expressing GFP (green) driven by the spiracle specific *ems-Gal4* line. (B) Spiracle cells overexpressing Cv-c with *ems-Gal4* show normal aPKC and neurotactin expression. GFP staining in (B) is less conspicuous than in (A) because of the membrane location of Cv-c-GFP. Arrows point to the apical region in the posterior spiracles. (C) Epidermal cells expressing Cv-c using *en-Gal4* as a driver lose aPKC except those of the leading edge (arrowheads). (D) Tracheal cells, labelled with anti-Trh (blue nuclei), do not lose aPKC (red) after Cv-c ectopic expression (arrowheads; compare with the decrease in nearby ectodermal cells, arrow). (E) Salivary gland cells do not lose aPKC localization after Cv-c ectopic expression. (F-I) Ectopic posterior spiracle Cv-c expression in heterozygous *crb* or *E-cad* embryos. Posterior spiracles of heterozygous mutants for *crb* (F, H) or the *E-cad* allele shg^{IH} (G, I) develop normally in control embryos expressing the mutant Cv-c^{R601Q} (F-G) while

frequently display invagination defects when expressing wild type Cv-c (H-I). Arrows in H and I point to spiracle cells that failed to invaginate and are not expressing aPKC and the homologous spiracle region in embryos expressing the mutated Cv-c form in F and G. F-F' and H-H' show two confocal sections of the same spiracle at different focal planes. (J) Ectopic Abd-B expression driven in the ectoderm with the *69B-Gal4* line forms supernumerary posterior spiracles (arrowheads) as detected with anti-Ct expression (blue), without affecting the cell polarity (aPKC red or grey, note the increased levels of aPKC in the spiracle lumen). (K) Close-up of panel J showing the ectopic spiracles formed in two segments. (L) Embryo simultaneously expressing Cv-c and Abd-B with the *69B-Gal4* line. Note the loss of aPKC from the anterior trunk segments except in the areas associated to the formation of ectopic posterior spiracles (Blue labels Ct expression in the ectopic spiracles, green Cv-c expressing cells, red or grey aPKC). (M) Close-up of panel L showing that aPKC expression remains associated to the ectopic posterior spiracles (arrowheads).

Scale bar: 100μm in (J) and 10μm in the rest of panels. In all panels dorsal is up and anterior is left.

Figure 5. Rescue of Cv-c induced polarity defects.

(A-D) Rescue of apically polarized protein localization in cells expressing Cv-c and Abd-B effectors. (A-B) Coexpression of RhoGEF2 (red in A and B) restores both E-Cad localization (A' and blue in A) and aPKC (B' and blue in B). (C) Expression of an aPKC-myc tagged protein in ectodermal cells restores aPKC (blue in C) and E-Cad membrane localization (C' and red in C). (D) Expression of E-Cad is unable to restore aPKC membrane localization (D' and red in D). (E) Both E-Cad and aPKC membrane

localization is rescued when Cv-c is coexpressed with Rab11 (red and blue in E and E' and E'' respectively).

(F-H) Increased Rab11 levels in the posterior spiracle depend on Abd-B. (F) Cross-section of a posterior spiracle (asterisk) in a wild type embryo shows higher protein levels of Rab11 in spiracle cells than in neighboring cells (arrowhead). Ectopic Abd-B expression with *69B-Gal4* increases Rab11 in all trunk segments (G, arrowheads) while increased Rab11 levels disappear in Abd-B mutant embryos (H, asterisk marks the position in A8 where the spiracle normally forms).

Scale bar: 10µm. In all panels dorsal is up and anterior is left. Panels A-E and G show Z-sections along the thin white lines and the asterisk in Z sections indicate the cells overexpressing Cv-c.

Supplementary Materials and Methods

Fly Stocks and Genetics.

Gene expression was induced with the *en-Gal4*, *69B-Gal4* and *ems-Gal4* driver lines. The following mutants were used: crb^{11A22}, $aPKC^{K06403}$ (Bloomington Drosophila Stock Center), $gef64C^{29}$ (1), $Abd\text{-}B^{M1}$ (2), shg^{IH} (3). The following lines were expressed: $UAS\text{-}RhoA^{V14}$, $UAS\text{-}RhoA^{N19}$, $UAS\text{-}Rac^{V12}$, $UAS\text{-}Rac^{DN}$ (4, 5), *UAS-DIAP1* (6), *UAS-Crb* (7), *UAS-E-Cad* (8), *UAS-Cv-c* (9), *UAS-Rab11* (Bloomington Drosophila Stock Center), *UAS-Cad86C* (10), *UAS-Cad74A* (11), *UAS-RFP-RhoGEF2* (12), *UAS-RhoGEF64C* (1).

Immunohistochemistry and Cuticle Preparations

Cuticle preparation was performed as described in Hu and Hombría (13).

Embryos were fixed as described in (14) and stained with the following antibodies: anti-Myc (Cell Signalling), anti-aPKC C20 (Santa Cruz Biotechnology), anti-Crb, anti-perlecan, anti-Mmp1, anti-Dlg, anti-E-Cad (Developmental Studies Hybridoma-Bank), anti-laminin (15), anti-active Caspase-3 (Cell Signalling), anti-Scribble (a gift from D. Bilder). Secondary antibodies were conjugated to Alexa 488, 555 and 647 (Invitrogen). Images were taken on a Leica SP2-AOBS microscope and processed using ImageJ and Adobe Photoshop. Fluorescent in situ hybridization was performed according to standard protocols adding a secondary fluorescence antibody (anti-goat Alexa 647); *cv-c* riboprobe was marked using DIG RNA Labeling Kit (Roche).

Time-lapse image collection

The embryos were mounted as described in Wood and Jacinto (16). Time-lapse images were taken with a Nikon Eclipse E800 microscope coupled to a BioRad MRC1024 confocal unit, with a 40X oil immersion objective. For each movie, twenty six to thirty

time points were collected. For each time point, between 20 and 40 *Z* sections were collected (spaced between 0.5 μm and 1 μm). Movies were assembled using ImageJ.

Cell size quantification

Average apical size was quantified in wild type cells or in *en-Gal4* cells expressing Cv-c-GFP or Cv-c^{R601Q}-GFP. Wild type anterior compartment cells have a cell width of 3.6μm (n=31), posterior compartment cells expressing Cv-c^{R601Q}-GFP 3.6μm (n=13) and Cv-c-GFP expressing cells have a 5.4μm (n=31) apical cell width.

Constructs

Mutation of Cv-c was generated by PCR from Cv-c venus cDNA clone in pENTER (17) as template, and subsequently cloned into pTWV or pTVW (UASt promoter, C-terminal or N-terminal Venus tag respectively – obtained from The Drosophila Gateway Vector Collection, Carnegie Institution of Washington, Baltimore, MD; www.ciwemb.edu/labs/murphy/Gateway%20vectors.html, using the Gateway technology (Invitrogen).

The oligonucleotides used were (5'-3'):

Cv-c R601-Qfor: GGAATTTTCCAGAAAAGCGGTGGAAAGTCGC

Cv-c R601-Qrev: GCGACTTTCACCGCTTTTCTGGAAAATTCC

Constructs were injected in *D. melanogaster* by Bestgene (USA) and the *Drosophila* Consolider-Ingenio 2007 transformation platform (Spain).

Supplementary References

1. Bashaw GJ, Hu H, Nobes CD, & Goodman CS (2001) A novel Dbl family RhoGEF promotes Rho-dependent axon attraction to the central nervous system midline in Drosophila and overcomes Robo repulsion. *J Cell Biol* 155(7):1117-1122.
2. Casanova J, Sanchez-Herrero E, & Morata G (1986) Identification and characterization of a parasegment specific regulatory element of the abdominal-B gene of Drosophila. *Cell* 47(4):627-636.
3. Tepass U*, et al.* (1996) shotgun encodes Drosophila E-cadherin and is preferentially required during cell rearrangement in the neurectoderm and other morphogenetically active epithelia. *Genes Dev* 10(6):672-685.
4. Luo L, Liao YJ, Jan LY, & Jan YN (1994) Distinct morphogenetic functions of similar small GTPases: Drosophila Drac1 is involved in axonal outgrowth and myoblast fusion. *Genes Dev* 8(15):1787-1802.
5. Lee T, Winter C, Marticke SS, Lee A, & Luo L (2000) Essential roles of Drosophila RhoA in the regulation of neuroblast proliferation and dendritic but not axonal morphogenesis. *Neuron* 25(2):307-316.
6. Lohmann I, McGinnis N, Bodmer M, & McGinnis W (2002) The Drosophila Hox gene deformed sculpts head morphology via direct regulation of the apoptosis activator reaper. *Cell* 110(4):457-466.
7. Wodarz A, Hinz U, Engelbert M, & Knust E (1995) Expression of crumbs confers apical character on plasma membrane domains of ectodermal epithelia of Drosophila. *Cell* 82(1):67-76.

8. Pacquelet A & Rorth P (2005) Regulatory mechanisms required for DE-cadherin function in cell migration and other types of adhesion. *J Cell Biol* 170(5):803-812.

9. Denholm B*, et al.* (2005) crossveinless-c is a RhoGAP required for actin reorganisation during morphogenesis. *Development (Cambridge, England)* 132(10):2389-2400.

10. Schlichting K & Dahmann C (2008) Hedgehog and Dpp signaling induce cadherin Cad86C expression in the morphogenetic furrow during Drosophila eye development. *Mechanisms of development* 125(8):712-728.

11. Lovegrove B*, et al.* (2006) Coordinated control of cell adhesion, polarity and cytoskeleton underlies Hox-induced organogenesis in *Drosophila*. *Curr Biol* 16:2206-2216.

12. Wenzl C, Yan S, Laupsien P, & Grosshans J (2010) Localization of RhoGEF2 during Drosophila cellularization is developmentally controlled by Slam. *Mechanisms of development* 127(7-8):371-384.

13. Hu N & Castelli-Gair J (1999) Study of the posterior spiracles of Drosophila as a model to understand the genetic and cellular mechanisms controlling morphogenesis. *Dev Biol* 214(1):197-210.

14. Sotillos S, Diaz-Meco MT, Moscat J, & Castelli-Gair Hombria J (2008) Polarized subcellular localization of Jak/STAT components is required for efficient signaling. *Curr Biol* 18(8):624-629.

15. Kumagai C, Kadowaki T, & Kitagawa Y (1997) Disulfide-bonding between Drosophila laminin beta and gamma chains is essential for alpha chain to form alpha betagamma trimer. *FEBS Lett* 412(1):211-216.

16. Wood W & Jacinto A (2005) Imaging cell movement during dorsal closure in Drosophila embryos. *Methods Mol Biol* 294:203-210.

17. Simoes S*, et al.* (2006) Compartmentalisation of Rho regulators directs cell invagination during tissue morphogenesis. *Development (Cambridge, England)* 133(21):4257-4267.

Supplementary Figure legends

Supplementary Figure 1. Endogenous epithelial expression of *cv-c*, aPKC, Crb and E-Cad. (A) *cv-c* RNA in a wild type stage 11 embryo showing expression in the tracheal pits and the leading edge cells. (B) *en-Gal4>UAS-GFP* embryo showing the posterior cells labelled by GFP and *cv-c* RNA expressed in the tracheal pits. (C) Close-up of B showing *cv-c* expression in the tracheal pit (tp) while the posterior cells (p, green) and adjacent anterior compartment cells (a) do not express *cv-c* (C'). (D-J) Anti-aPKC, (K-P) anti-Crb and (Q-V) anti-E-Cad staining of embryos at stage 11 (D-E, K-L, Q-R), stage 13 (F-H, M-N, S-T) and stage 14 (I-J, O-P, U-V). Note the higher protein levels in tracheal pits, leading edge and posterior spiracles, domains where *cv-c* is also expressed. Scale bar: 10μm. In all panels dorsal is up, ventral is down, anterior is left and posterior is right.

Supplementary Figure 2. Cuticles of embryos expressing Cv-c and activated or dominant negative Rho1 under the control of *en-Gal4*. (A) Cv-c expression causes holes probably due to abnormal cuticle secretion and not to cell death as the same phenotypes are observed in combination with DIAP1 (D). (B) Expression of a constitutive active form of Rho1 causes head defects and dorsal puckering due to dorsal closure defects during embryogenesis. (C) Combination of both transgenes exhibits the $Rho1^{V14}$ phenotype indicating Cv-c defects are due to Rho1 inactivation. (E) Expression of the dominant negative $Rho1^{N19}$ produces cuticles with holes similar to those caused by Cv-c expression. (F) Simultaneous expression of $Rho1^{N19}$ and Cv-c causes similar holes to those caused by the separate expression of each protein. Scale bar: 10μm. In all panels anterior is left.

Supplementary Figure 3. Rac does not mediate ectopic Cv-c expression phenotypes. (A-D) Epidermis of stage 14-15 embryos expressing the indicated UAS lines is under the control of *en-Gal4* (aPKC red, Dlg blue, Cv-c green). Z-sections along the white thin line are shown below. (E-H) Cuticles secreted by embryos of the same genotypes as those shown in the panels above. (A) Expression of a constitutive activated form of Rac does not affect cell polarity, and the cuticle (E) does not form holes. (B) Active Rac^{V12} does not rescue Cv-c effects on apical polarity markers nor the cuticle holes (F). (C) Expression of a dominant-negative form of Rac does not affect apical markers, and the cuticles do not have holes (G). (D) Coexpression of dominant negative Rac and Cv-c shows the apical polarity defects and cuticle holes (H) caused by Cv-c. Scale bar: 10μm. Panels oriented as in previous figures.

Supplementary Figure 4. Quantification of aPKC levels in ectopic Cv-c expressing cells.

A representative example of a quantified embryo (A) expressing ectopic Cv-c-GFP (green) with the *en-Gal4* line and stained with aPKC (red) . Single channel images of the aPKC (B) and Cv-c-GFP (C) stainings shown in panel (A). Short lines labelled D to G in panels (B-C) indicate membrane sites where the protein levels were quantified. Quantification was done using Image J software. Measurements at similar positions were taken from cells localized in the leading edge of either Cv-c expressing (graph E) or non-expressing (graph D) cells; as well as in more ventral epithelia of either Cv-c expressing (graph G) or non-expressing cells (graph F).

(D-G) Graphs show fluorescence levels for aPKC (red) and Cv-c-GFP (blue) across the cell. 10 confocal images of 0.16 μm thickness comprising the aPKC expression domain were projected using the average intensity algorithm. Three cell pairs were selected randomly and the fluorescence level (pixel grey intensity in arbitrary units) for aPKC (red) and Cv-c (blue) was measured along a 2,5 μm line with the apposing cell membranes at its centre.

Scale bar 10μm.

Supplementary Figure 5. Abd-B compensates Rho1DN defects.

Expression of Abd-B rescues Rho1DN epithelial defects in the areas associated to the formation of ectopic spiracles as shown by aPKC staining (A' and red in A, asterisks). Green labels Ct expression in the ectopic spiracles.

Scale bar: 10µm. Z-sections along the thin white lines.

Supplementary Figure 6. Expression of Abd-B targets in cells where ectopic Cv-c defects were rescued by Abd-B activation. Ectopic Cv-c and Abd-B expression driven in the ectoderm with the *69B-Gal4* line in embryos carrying the posterior spiracle specific enhancer *ems-lacZ 0.35*. Ectopic posterior spiracles (arrowheads) are detected by the expression of ßGal (blue). Note that Abd-B expression induces high levels of E-Cad (red in A-B and grey A'-B') and Rab11 (red in C-D and grey C'-D'). B and D are close ups showing Z-sections along the thin white lines. Scale bar: 10µm.

Movie 1. Time-lapse movie of embryos expressing GFP in the posterior compartments. In en-Gal4/+; UAS-GFP/+ embryos, wild-type posterior compartment

cells maintain their relative positions. All posterior compartments are separated by non-GFP expressing anterior compartment cells.

Movie 2. Time-lapse movie of embryos expressing Cv-c-GFP in the posterior compartments. In en-Gal4/+; UAS-cv-cGFP/+ embryos, Cv-c GFP expressing cells are motile and in some cases the posterior compartment cells in one segment may contact the posterior compartment cells from a neighbouring segment.

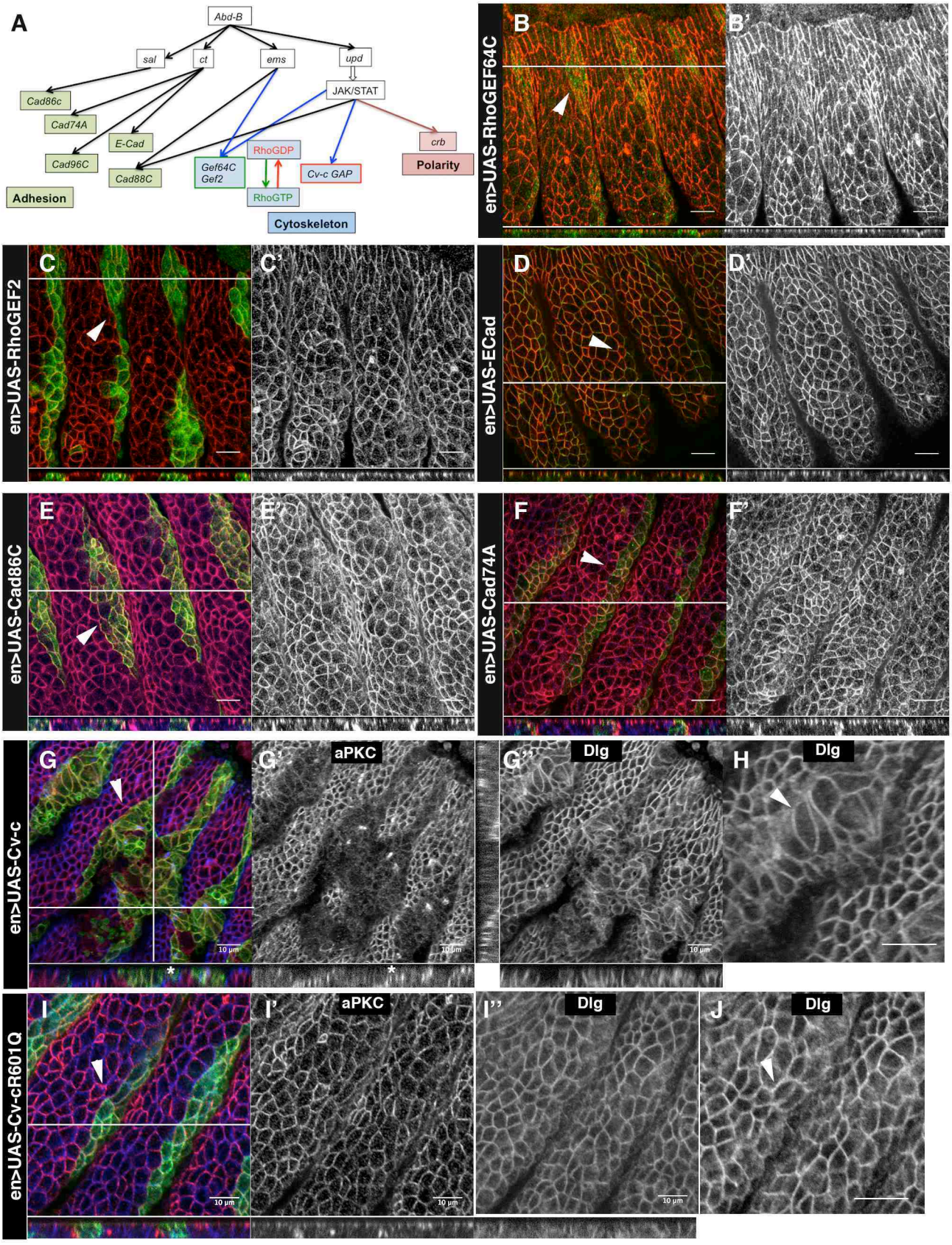

Figure 1. Sotillos et al.

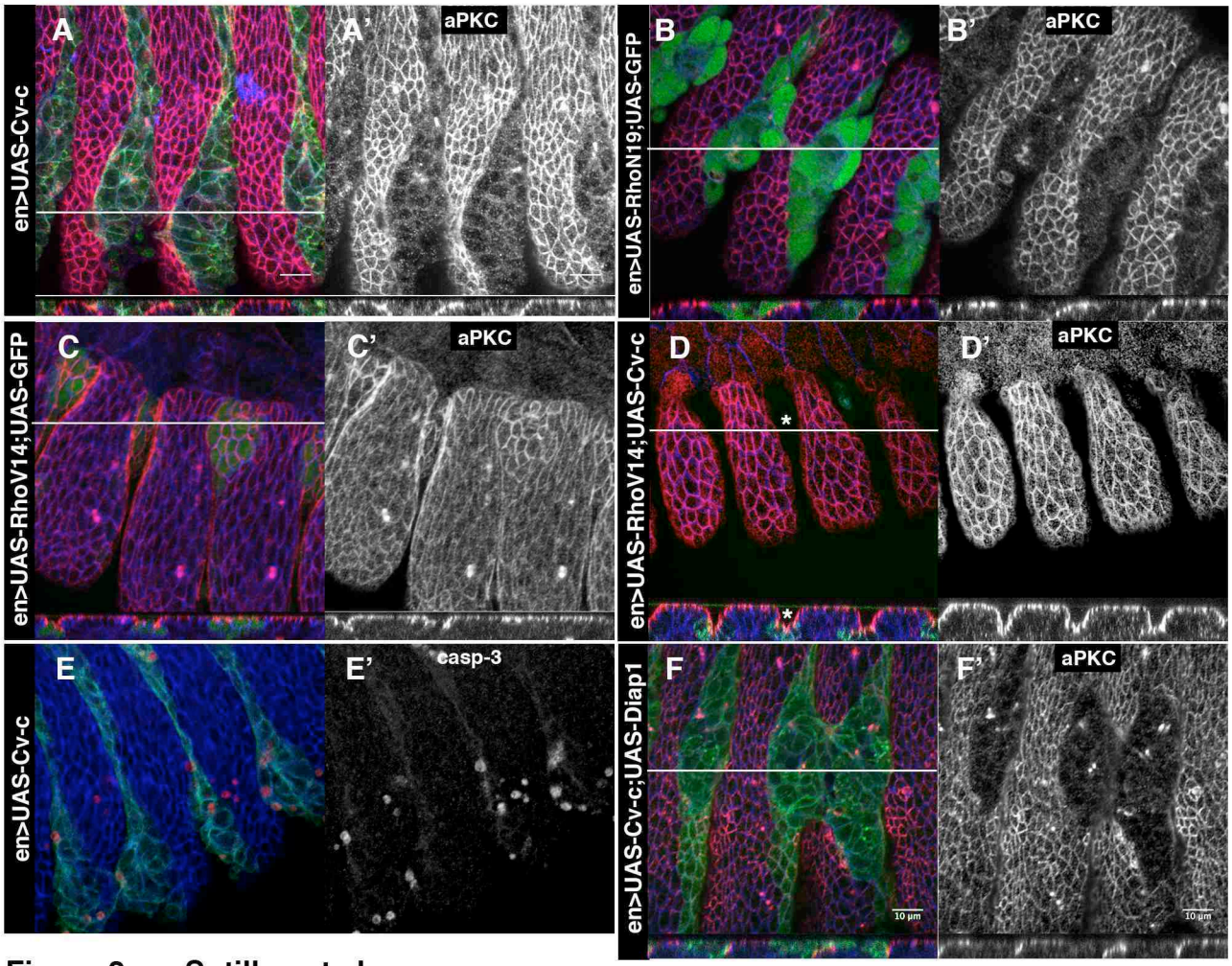

Figure 2 **Sotillos et al.**

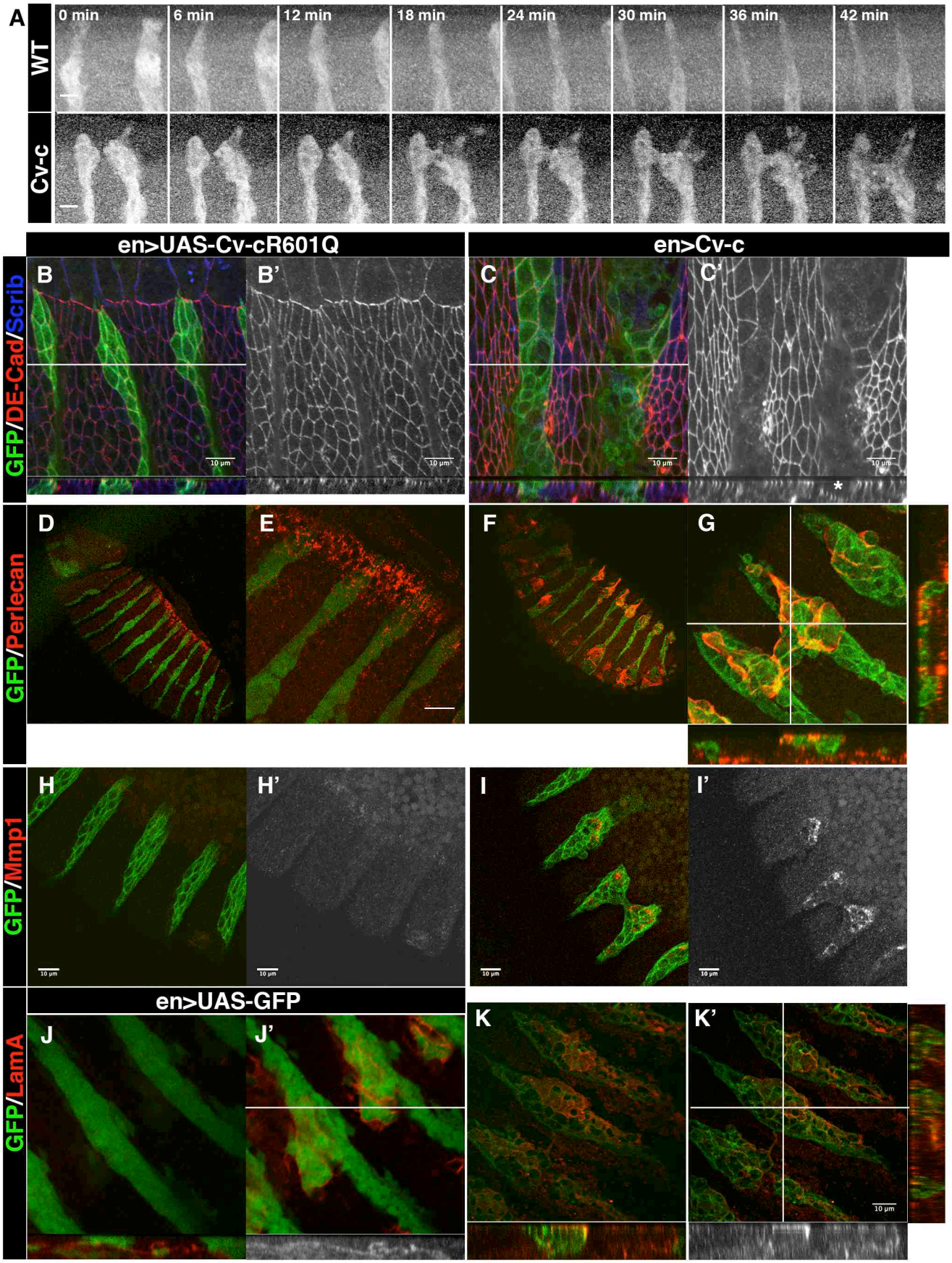

Figure 3 Sotillos et al.

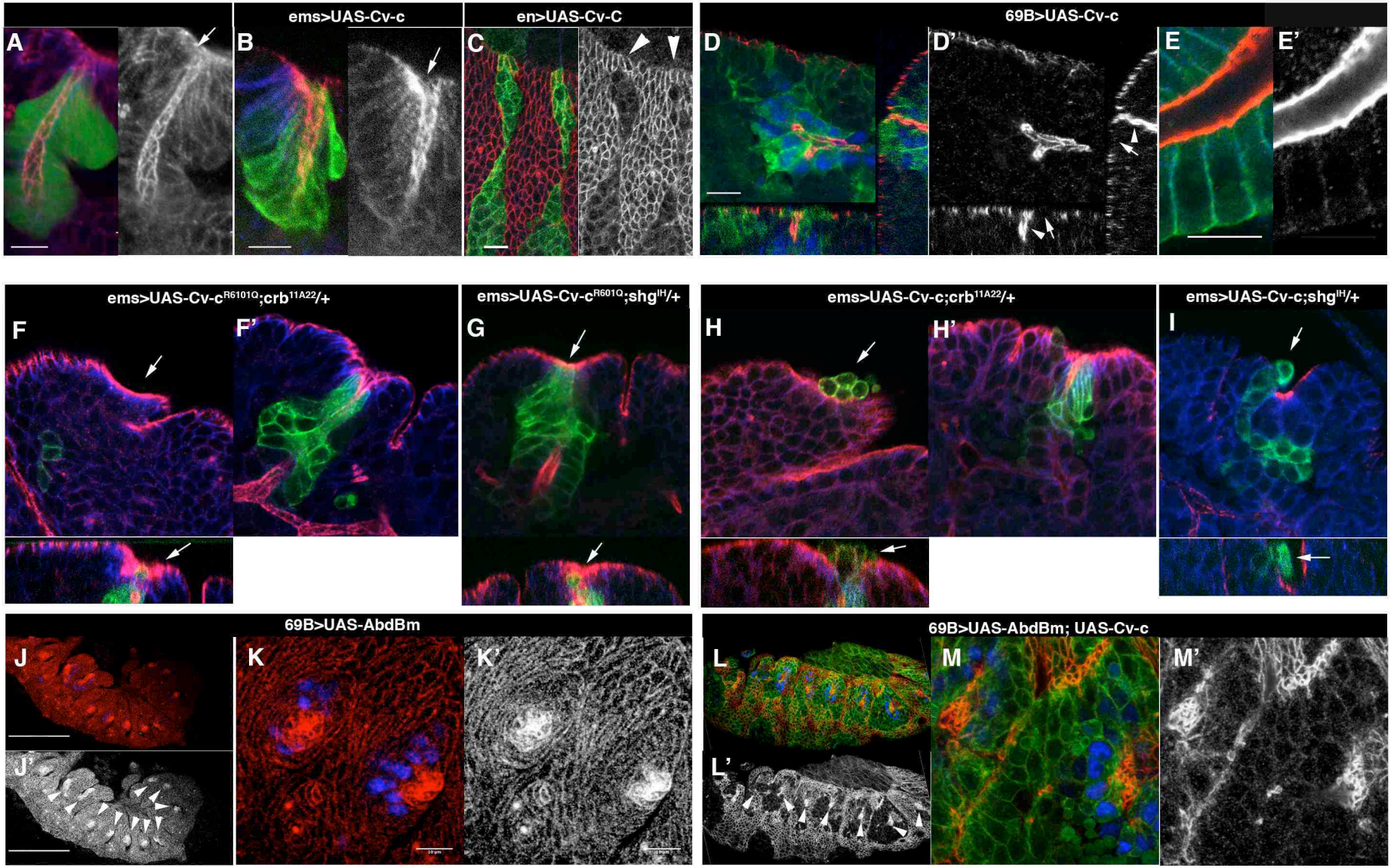

Sotillos et al. Figure 4

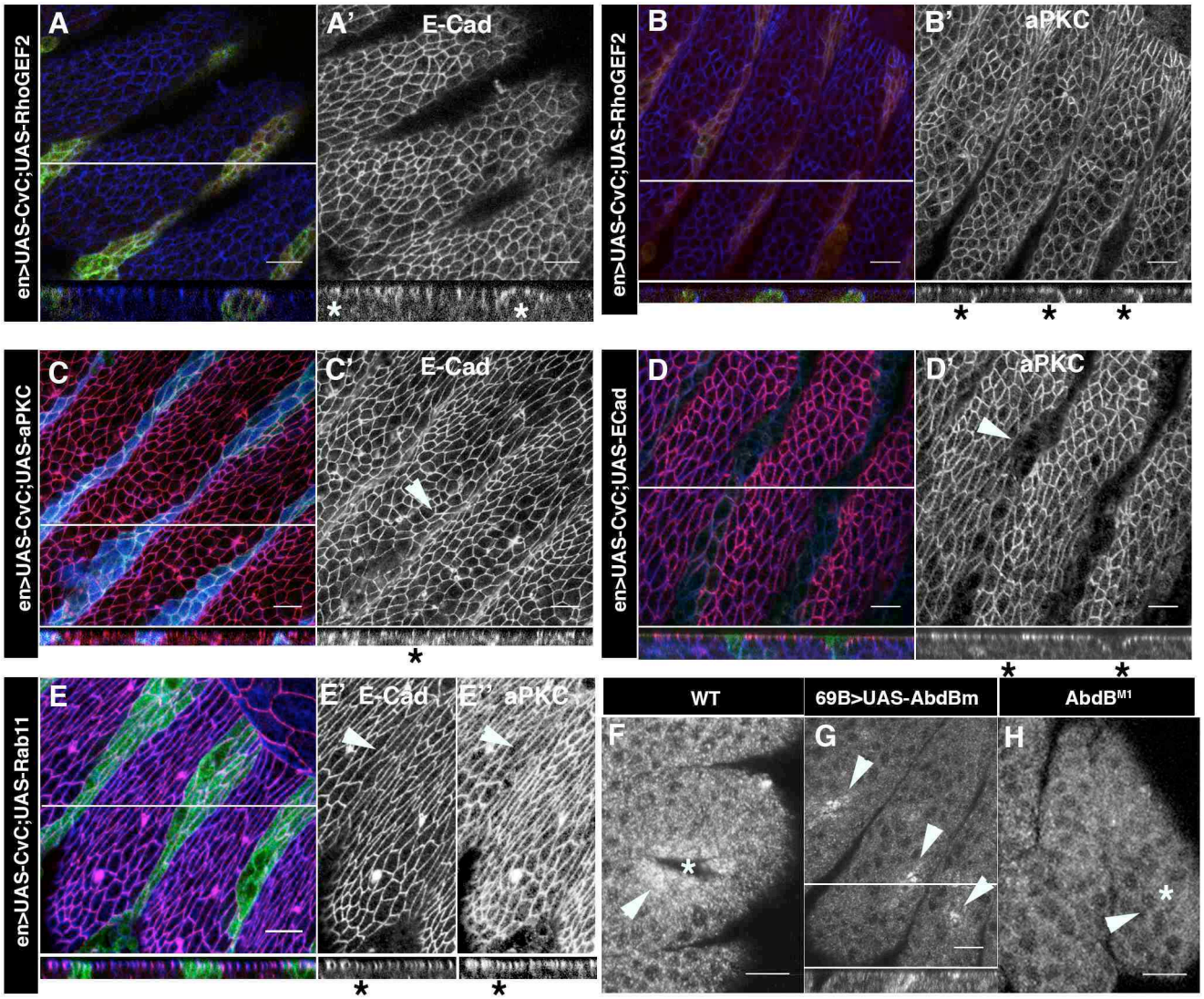

Figure 5 Sotillos et al.

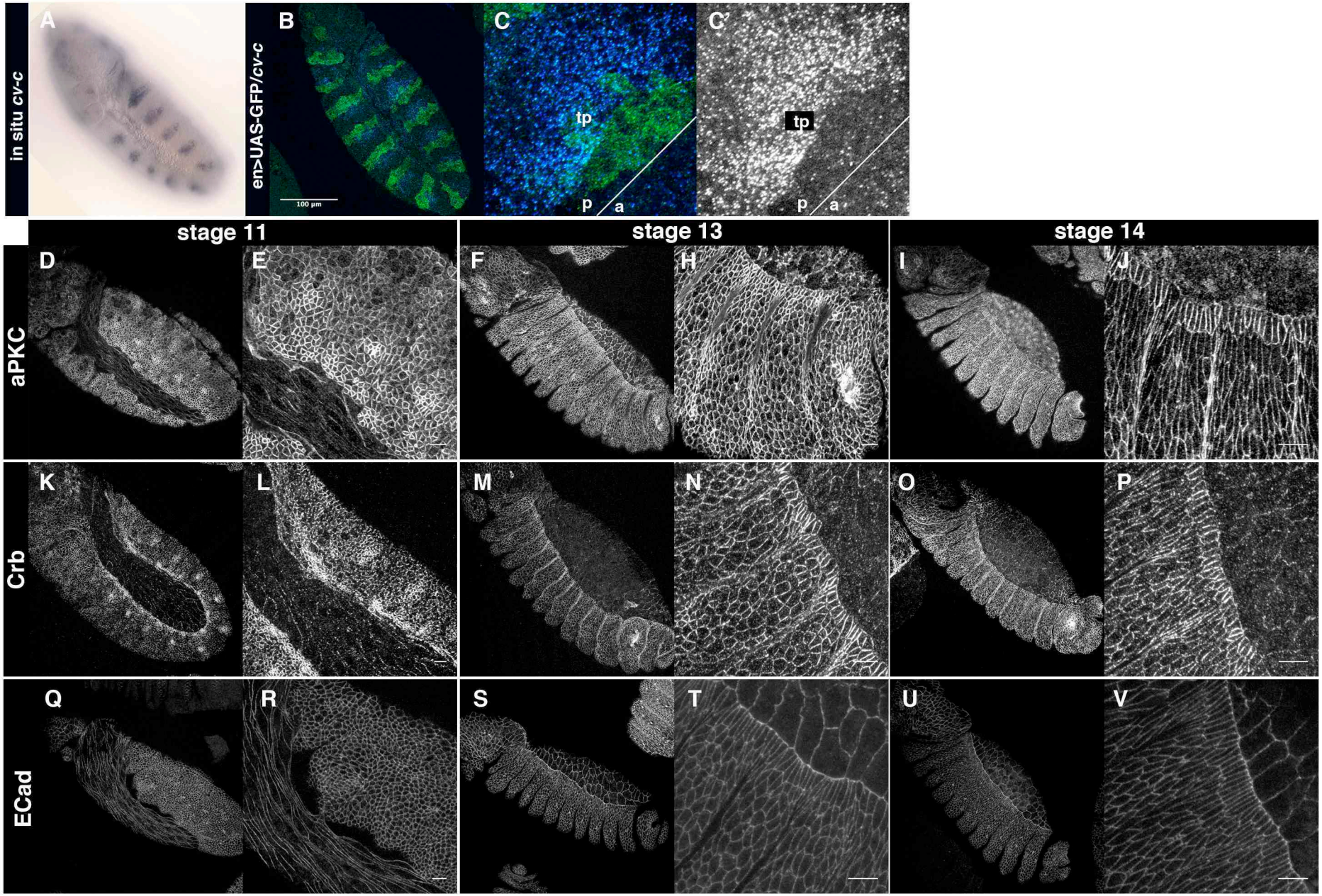

Supp. Figure 1 Sotillos et al.

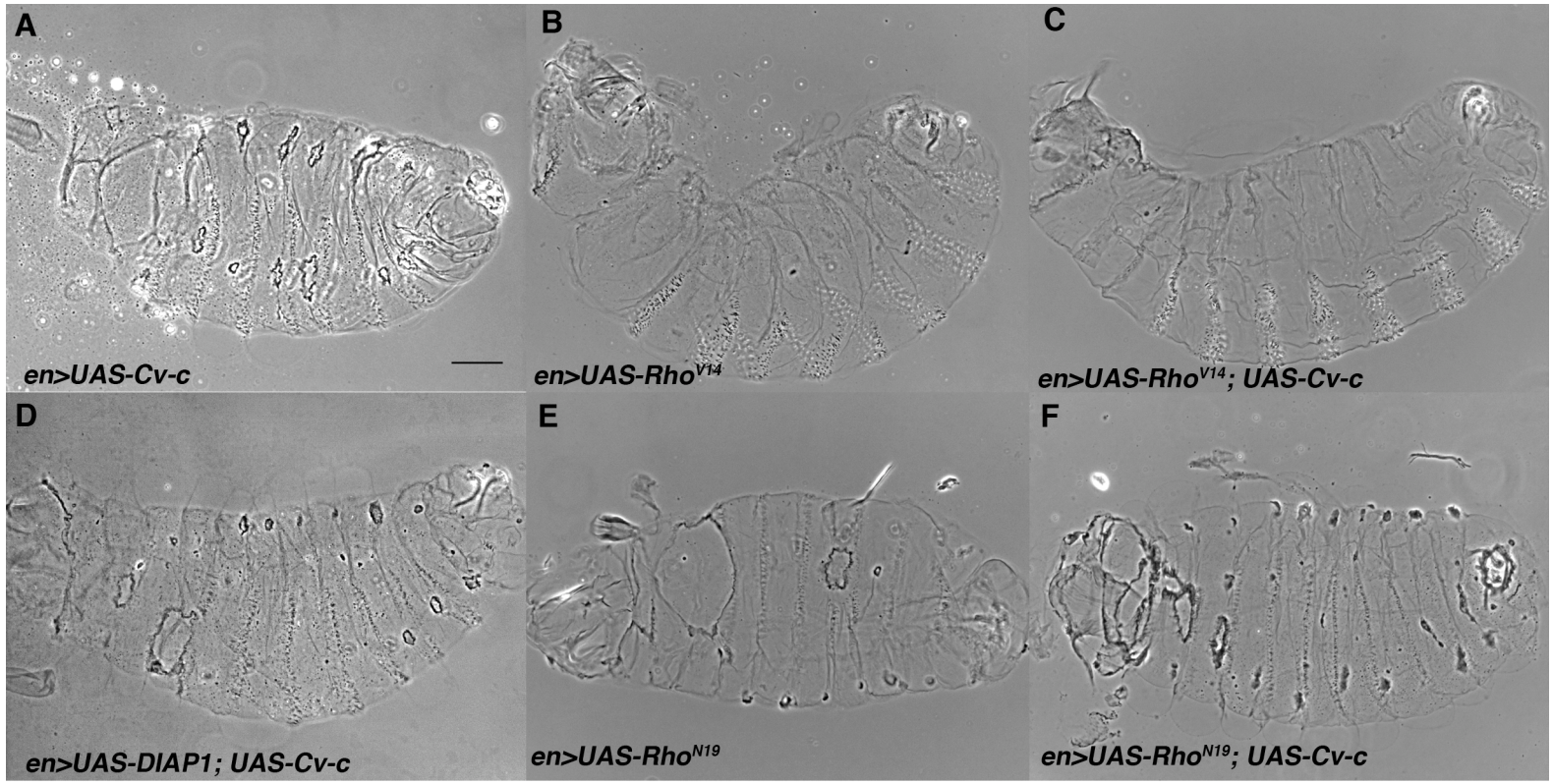

Supp. Figure 2 Sotillos et al.

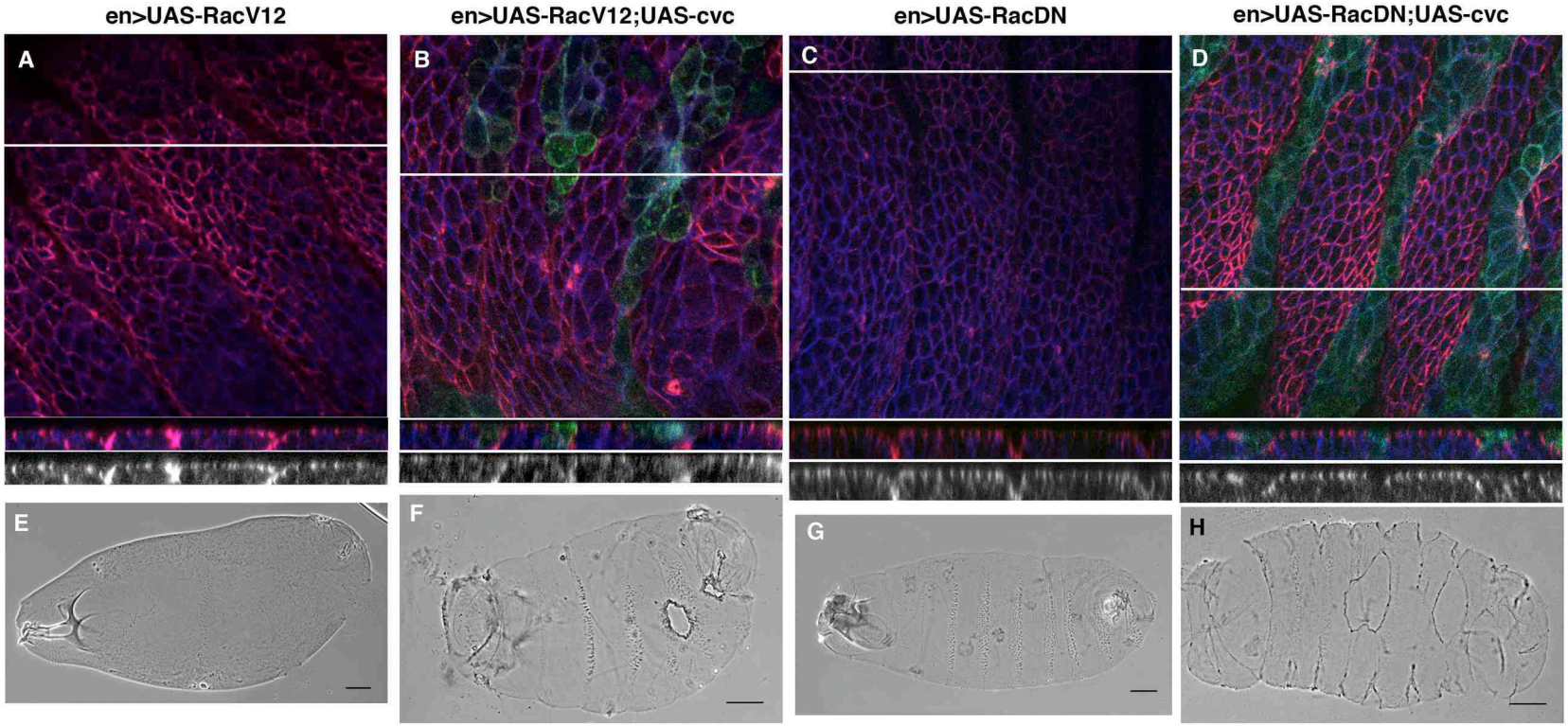

Supp. Figure 3 Sotillos et al.

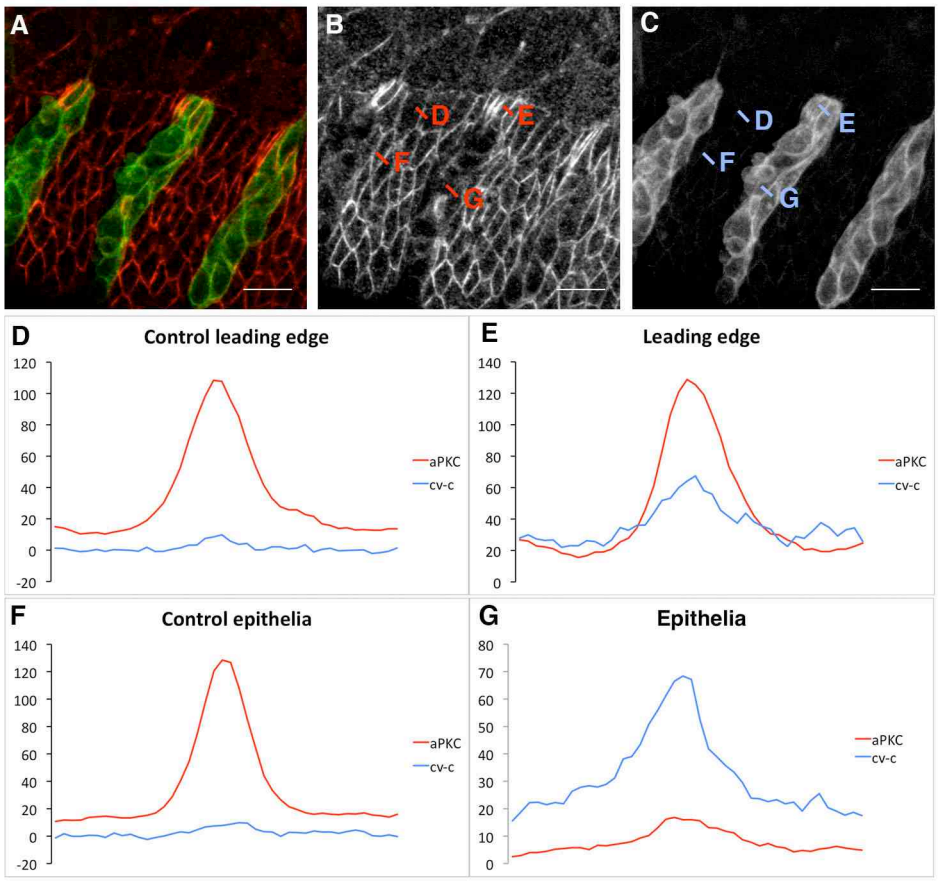

Supplementary Fig 4 Sotillos et al

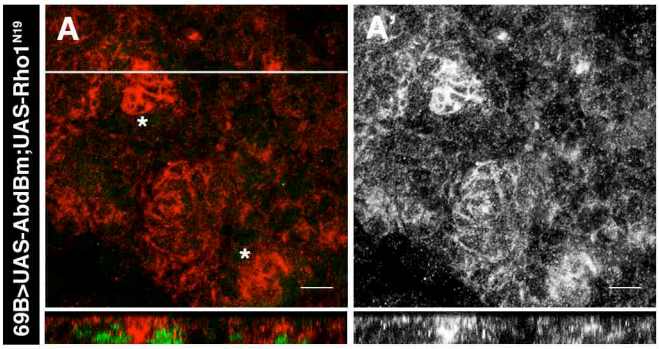

Supp. Figure 5 Sotillos et al.

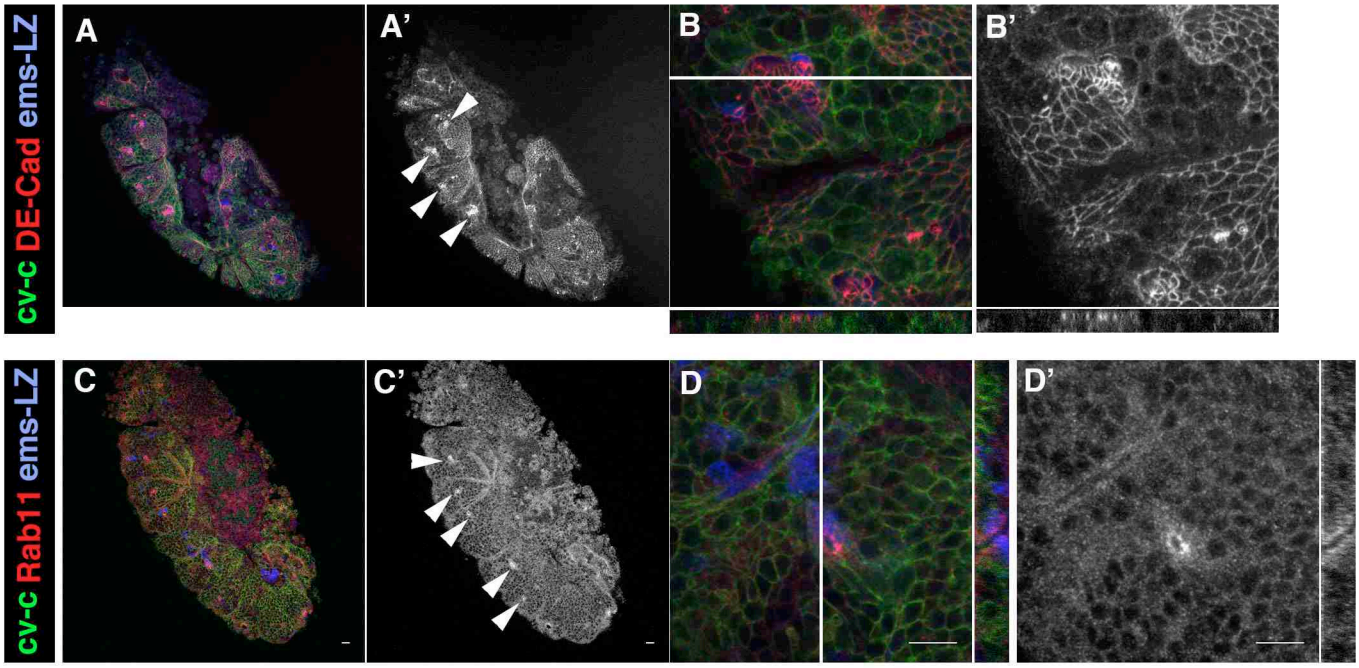

Supp. Figure 6 Sotillos et al.